



ISTITUTO NAZIONALE DI RICERCA METROLOGICA Repository Istituzionale

Piston provers dead volume evaluation

Original

Piston provers dead volume evaluation / Spazzini, Pier Giorgio; Piccato, Aline. - In: MEASUREMENT. - ISSN 0263-2241. - 259:B(2026). [10.1016/j.measurement.2025.119633]

Availability:

This version is available at: 11696/88439 since: 2026-02-27T12:53:02Z

Publisher:

Elsevier

Published

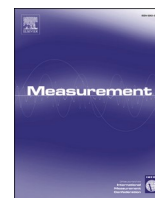
DOI:10.1016/j.measurement.2025.119633

Terms of use:

This article is made available under terms and conditions as specified in the corresponding bibliographic description in the repository

Publisher copyright

(Article begins on next page)



Piston proves dead volume evaluation[☆]

Pier Giorgio Spazzini , Aline Piccato ^{*} 

INRIM, Torino, Italy

ARTICLE INFO

Keywords:

Dead Volume
Piston prover
Uncertainty

ABSTRACT

In piston prover measurements, the term “dead volume” denotes the portion of internal space that remains unreachable by the piston during operation. This volume includes not only the lateral sections of the containing cylinder but also the bottom of the cylinder, as well as auxiliary components such as connecting tubing and recessed areas designed to accommodate measurement instruments. The presence of this volume plays a critical role, as it directly affects the accuracy of the measurements obtained with the device.

Specifically, in INRIM facilities where the mass balance method is applied—calculating gas quantity variation by the difference between the estimated gas mass at the beginning and end of a test—having a precise estimate of the initial volume, which inherently includes the dead volume, is essential. However, traditional geometric methods for assessing this volume, based on dimensional measurements, introduce a significant degree of uncertainty.

To overcome these limitations, our laboratory has developed an innovative approach that involves injecting a known and controlled amount of gas, measured through the integration of flow data from a calibrated mass flow controller (MFC), and then analyzing the resulting changes in thermodynamic conditions within the piston chamber. This method enables a more accurate characterization of the dead volume, thereby reducing the uncertainty associated with its evaluation. A detailed uncertainty budget analysis for our Microgas and MeGas test facilities will also be presented. In this article, the Authors extend the investigation on the topic of dead volume in piston provers published in the Proceedings of the XXIV IMEKO World Congress [1].

1. Introduction

INRIM conducts primary reference measurements of gas flow rate using three test rigs: one bell prover and two piston provers. Each system operates in two distinct modes—intake, where gas flows into the accumulating volume, and delivery, where gas exits the accumulating volume. The technical specifications and validated metrological performance of these systems are comprehensively documented in the literature (see, e.g., [2–6]) Table 1a.

All measurements fundamentally rely on the mass balance principle. Specifically, the gas mass within the containment volume is estimated at both the start and end of the measurement interval. The difference between these two mass values yields the net gas mass variation, which can be used to calculate either the total gas quantity or, when divided by the measurement duration, the gas flow rate. Although this discussion will focus primarily on piston provers, the underlying methodology is essentially identical for bell-type provers Table 1b.

The initial gas mass is determined by multiplying the gas density—derived from measured thermodynamic conditions—by the initial internal volume. This initial volume consists of two components: the piston displacement volume and the dead volume. The dead volume corresponds to the portion of the cylinder’s internal space that remains unoccupied by the piston even at its lowest position. Similarly, the final gas mass is calculated by multiplying the density at the end of the measurement by the final internal volume, obtained by adding the piston displacement during the measurement to the initial volume Table 1c.

The dead volume is a critical contributor to the measurement uncertainty budget. Its influence depends on the magnitude of the dead volume itself, its associated uncertainty, and the difference between the initial and final thermodynamic states. The overall impact on the test rig’s total uncertainty is relatively small due to the comparatively low sensitivity of the system to this uncertainty component, but depending on the conditions it can have an influence; more details are provided in Sec. 5.3 Table 2.

[☆] This article is part of a special issue entitled: ‘MEASUR_XXIV IMEKO World Congress’ published in Measurement.

^{*} Corresponding author at: c/o INRIM, Strada delle Cacce 91, Torino 10135, Italy.

E-mail addresses: p.spazzini@inrim.it (P.G. Spazzini), a.piccato@inrim.it (A. Piccato).

Table 1a

Uncertainty balance for the determination of the dead volume, small piston prover.

Source	Uncertainty (%)	Distribution	Contribution (%)
V_{add}	0.2	Gaussian	0.2
$\frac{P_{\text{ref}}}{T_{\text{ref}}}$	0	Gaussian	0
T_f	0.009	Gaussian	0.009
p_f	0.005	Gaussian	0.005
$\frac{1}{1 - \frac{p_i}{p_f} \cdot \frac{T_f}{T_i}}$	0.73	Gaussian	0.73
Total	–	–	0.76

Table 1b

Uncertainty balance for the determination of the dead volume, large piston prover.

Source	Uncertainty (%)	Distribution	Contribution (%)
V_{add}	0.2	Gaussian	0.2
$\frac{P_{\text{ref}}}{T_{\text{ref}}}$	0	Gaussian	0
T_f	0.017	Gaussian	0.009
p_f	0.015	Gaussian	0.015
$\frac{1}{1 - \frac{p_i}{p_f} \cdot \frac{T_f}{T_i}}$	1,17	Gaussian	1.17
Total	–	–	1.19

Table 1c

Experimental results and associated uncertainties, all tests, small piston case.

Test #	Computed Volume (mL)	Expanded uncertainty (%)	Expanded uncertainty (mL)
1	261.70	0.76	1.98
2	243.24	0.75	1.83
3	261.26	0.76	1.99
4	242.61	0.75	1.82
5	260.38	0.77	2.00

Table 2

Experimental results and associated uncertainties, all tests, large piston case.

Test #	Computed volume (L)	Expanded uncertainty (%)	Expanded uncertainty (L)
1	454.77	1.22	5.55
2	453.62	1.22	5.53

Importantly, the dead volume cannot be eliminated due to its intrinsic origin in essential mechanical design features, such as sensor housings, pressure tubing connections, mechanical clearances, and safety spacers. Nonetheless, careful design efforts aim to minimize this volume where possible.

Currently, dead volume estimation in our piston provers is based on geometric analysis, which involves calculating volumes from the design dimensions of individual components. However, this approach introduces significant uncertainty arising from simplifying assumptions and manufacturing tolerances. In general, this is not a big issue, since the principle of the piston prover is such that the effect of the dead volume is relatively small; on the other hand, when very low uncertainties are sought, in some cases this contribution can have a measurable effect on the overall uncertainty; an example of such situation is described in Par. 4.3 and detailed in Tables 3 and 4. The advantage of the methodology presented here is that it allows a reduction in the uncertainty associated with the dead volume with relatively low effort, provided the measurements of the thermodynamic conditions are very accurate.

Besides geometric analysis, other commonly used methods for

Table 3

Current uncertainty balance for the small piston prover (large variation of density scenario).

Quant.	Typical value	Standard unc.	Sensit. coeff.	Contribution to overall St. unc.
p	100 KPa	0,0016 %	1	0,0016 %
T	293 K	0,003 %	1	0,003 %
ΔV	500 mL	0,0103 %	1	0,0103 %
V_I	262 mL	3 %	0,004	0,012 %
t	60 s	0,002 %	1	0,002 %
M_{mol}	28,0137 Kg/ kmol ⁻¹	0,003 %	1	0,003 %
Total	--	--	--	0,0165 %

Table 4

Revised uncertainty balance for the small piston prover (large variation of density scenario).

Quant.	Typical Value	Standard Unc.	Sensit. Coeff.	Contribution to overall St. Unc.
p	100 KPa	0,0016 %	1	0,0016 %
T	293 K	0,003 %	1	0,003 %
ΔV	500 mL	0,0103 %	1	0,0103 %
V_I	262 mL	1 %	0,004	0,004 %
t	60 s	0,002 %	1	0,002 %
M_{mol}	28,0137 Kg/ kmol ⁻¹	0,003 %	1	0,003 %
Total	--	--	--	0,0121 %

inventory volume (and consequently dead volume) determination include:

Pressure-decay methods, which estimate volume based on the rate of pressure change within a sealed system. These methods are sensitive to measurement precision and are often employed in leak testing and permeability studies [7].

Expansion methods, where a known volume of gas expands into an unknown volume, allowing calculation of the unknown volume from pressure and temperature changes [8].

It is also worth highlighting that the issue of dead volume—and the resulting uncertainty—is not unique to piston provers. Similar challenges arise in other measurement systems, as reported in the literature [9,10] and further discussed by Wright et al. [11]. Consequently, the methodology proposed herein for dead volume assessment may be applicable beyond the specific context of piston provers.

2. Experimental setup

2.1. Small test rig and associated instruments – Microgas

The first experimental measurements were carried out using INRIM's compact piston prover (Microgas) [3,4,5], which is a plunger-type test rig with a total volume capacity of about 3000 mL and highly precise temperature regulation.

Piston displacement is tracked by an interferometer with an overall accuracy better than 0.5 μm , while the piston diameter is traceable to the SI standard with an uncertainty of 2.5 μm . A differential pressure sensor is also connected to the cylinder, with its reference port exposed to the atmosphere. Under normal test rig conditions, this sensor feeds the piston control system to maintain the cylinder pressure equal to atmospheric pressure. For extremely low flow rate measurements, which involve longer durations, atmospheric pressure fluctuations could affect accuracy; in such cases, the piston pressure control is based on barometer readings, ensuring the internal pressure stays fixed at a pre-determined setpoint. The current estimated dead volume is 262 mL with a 3 % uncertainty, approximately 7.9 mL. This test rig is regularly employed to calibrate flow meters operating over a range from 0.1 to about 1500 mL/min, achieving accuracies as tight as 0.05 %. Piston

pressure is measured by a RUSKA series 6200 barometer, calibrated at INRIM's pressure laboratory, which ensures a pressure measurement uncertainty of 5 Pa. Temperature measurements are conducted using two PT100 sensors installed in specially designed cavities within the cylinder wall, connected to a CORRADI 7000 thermometer. This temperature measurement system is calibrated at INRIM's temperature laboratory and offers an overall accuracy of 0.015 K. These instruments provide the initial and final thermodynamic parameters required for the calculations outlined in Section 3. Fig. 1 shows an image of the test rig set up in its standard configuration.

2.2. Large test rig and associated instruments – MeGas

In order to expand the analysis of the applicability of the method, another set of measurements was performed on INRIM's large piston prover (MeGas). Also in this case, the device is a plunger piston type, but in this case the diameter of the piston is of 1 m, with a possible run of approximately 1.2 m, providing therefore a working volume in the order of 1000 L. The total internal volume of the prover is about 1500 L when the piston is in its upper rest position, while the dead volume with the piston at its lowermost position is estimated at 465 L with an uncertainty of 3 % (≈ 14 L), based on geometrical considerations. The piston is made of a 1000 mm diameter, 1630 mm long, 14 mm thick carbon-steel cylinder, chromium plated, ground, and polished on its external surface. It is attached to a massive bottom flange and is vertically actuated by a finely controlled brushless motor mounted on a platform approximately 6 m high. The piston is driven by a finely controlled brushless motor through a gearbox and a lead screw; its movement is measured by an encoder fitted on the lead screw, and its accuracy was measured to be in the order of 1 μ m, while the diameter of the piston is traceable to the SI with an uncertainty of 42 μ m [6]. The piston moves inside a rigid but mechanically unfinished cylindrical chamber with an internal diameter of 1095 mm. A Teflon-coated 1000 mm O-ring gasket, compressed by an adjustable upper flange, ensures a leak-proof seal at the top of the chamber. The chamber rests on a 1950 mm diameter base, which has a 100 mm bore at its center connected to a bent pipe that conveys the gas displaced by the piston towards the test line. A group of automatically operated valves (including a safety valve, an air admission valve, and a

gas delivery valve) control the flow at the facility exit. Within the clearance between the piston and the chamber wall, 10 platinum resistance temperature sensors (PT100) are installed at different heights and circumferential positions to measure the average gas temperature and detect possible non-uniformities; the estimate for the (average) temperature uncertainty is of 0.025 K. The temperature sensing system is calibrated at INRIM's temperature laboratory. The pressure within the piston is measured by a suitable barometer, calibrated at INRIM pressure laboratory, that allows an uncertainty on measured pressure lower than 5 Pa. Unlike the Microgas facility, the MeGas system does not rely on a differential pressure sensor for pressure regulation; instead, it uses the barometric reference directly for pressure control. Considering the necessary piston acceleration, deceleration, and safety stroke margins, the largest gas volume that can be displaced and measured is approximately 800 L. The test rig is used for the calibration of flow meters at flow rates ranging from 5 to ≈ 500 L/min with an accuracy as low as 0.1 %. As in the previous case, the initial and final thermodynamic conditions were measured using the instruments associated with the test rig, described earlier. Fig. 2 shows the test rig in its usual configuration.

3. Principle of the method

The method we propose for determining the dead volume within a piston prover leverages the compressibility properties of gases and relies on precise measurements of thermodynamic parameters such as pressure and temperature.

When the prover is sealed and the piston remains stationary, injecting a known quantity of gas via a calibrated flow controller induces measurable changes in pressure and temperature. These changes can be related to the volume to be determined—the dead volume.

a) Fundamental Model

The starting point is the ideal gas law, expressed as:

$$p_a V_a = n_a R^* T_a \quad (1)$$

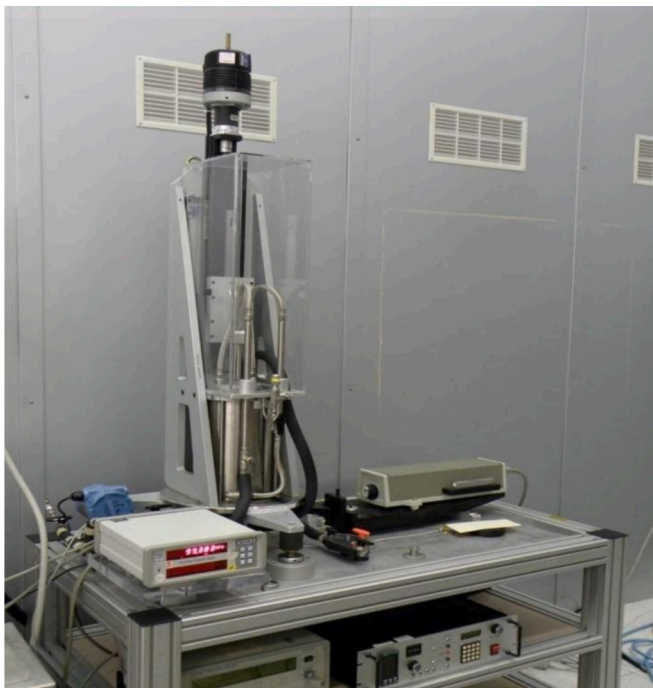


Fig. 1. Small piston prover (Microgas), typical setup.



Fig. 2. Large piston prover at INRIM, typical configuration.

where:

- p_α = pressure.
- V_α = volume.
- n_α = number of moles of gas
- R^* = specific gas constant.
- T_α = temperature.

Initially, at thermal equilibrium and before gas injection (denoted with subscript), the system satisfies:

$$p_i V_i = n_i R^* T_i \quad (2)$$

After injecting a known quantity of gas and allowing the system to stabilize, the new thermodynamic state (subscript f) is:

$$p_f V_f = n_f R^* T_f \quad (3)$$

Since the piston is held stationary during this process, the volume remains constant: $V_i = V_f$

Also, the gas constant R^* remains unchanged as the gas composition is constant.

b) Relating Initial and Final States.

Dividing Eq. (2) by Eq. (3) yields:

$$\frac{p_i V_i}{p_f V_f} = \frac{n_i R^* T_i}{n_f R^* T_f} \Rightarrow \frac{p_i}{p_f} = \frac{n_i T_i}{n_f T_f}$$

Rearranging to isolate n_i :

$$\frac{n_i}{n_f} = \frac{p_i}{p_f} \cdot \frac{T_f}{T_i} \Rightarrow n_i = n_f \cdot \frac{p_i}{p_f} \cdot \frac{T_f}{T_i} \quad (4)$$

c) Quantity of Gas Added

The gas added, quantified by the number of moles n_{add} , is determined by integrating the calibrated mass flow controller (MFC) output. The MFC reports flow in standard cubic centimeters per minute (SCCM), which correspond to specified reference thermodynamic conditions (p_{ref} , T_{ref}).

$$n_{add} = \frac{V_{add} p_{ref}}{R^* T_{ref}} \quad (5)$$

Using the ideal gas equation solved for n , the number of moles added can be calculated as: where V_{add} is the volume of gas added at the reference conditions.

By conservation of mass:

$$n_{add} = n_f - n_i \quad (6)$$

Substituting Eqs. (4) and (5) into (6) gives:

$$\frac{V_{add} p_{ref}}{R^* T_{ref}} = n_f - n_f \cdot \frac{p_i}{p_f} \cdot \frac{T_f}{T_i} = n_f \left(1 - \frac{p_i}{p_f} \cdot \frac{T_f}{T_i} \right) \quad (7)$$

d) Solving for Volume

Rearranging Eq. (7) to isolate n_f :

$$n_f = \frac{V_{add} p_{ref}}{R^* T_{ref}} \cdot \frac{1}{1 - \frac{p_i}{p_f} \cdot \frac{T_f}{T_i}} \quad (7a)$$

Substituting n_f back into Eq. (3) and plugging in n_f from (7a) the dead volume V can be expressed as follow:

$$V = \frac{R^* T_f}{T_i} \cdot \frac{V_{add} p_{ref}}{R^* T_{ref}} \cdot \frac{1}{1 - \frac{p_i}{p_f} \cdot \frac{T_f}{T_i}} = V_{add} \cdot \frac{p_{ref}}{T_{ref}} \cdot \frac{T_f}{p_f} \cdot \frac{1}{1 - \frac{p_i}{p_f} \cdot \frac{T_f}{T_i}} \quad (8)$$

e) Interpretation

Eq. (8) provides the volume V , which corresponds to the dead volume of the piston prover, expressed as a function of the known injected volume V_{add} , the reference thermodynamic conditions, and the

measured pressures and temperatures before and after gas injection.

4. Measurement procedure and uncertainty estimate

4.1. Procedure for the added volume measurement

The following measurement procedure for the added volume applies equally to both the Microgas and Megas piston provers. The volume increase was quantified using an MKS Mass Flow Controller (MFC) with a maximum flow capacity of 5 SCCM for the Microgas and 20,000 SCCM/20 SLM for the Megas, operated through dedicated control software. This software enabled the configuration of MFC parameters, the setting of steady-state flow rates, initiation of the flow, and continuous recording of the instrument output at defined time intervals.

Prior to experimentation, the MFC underwent a rigorous calibration process using the respective test rigs as reference standard. These calibrations followed a standardized protocol involving seven calibration points, each repeated three times to ensure reliability.

For precise curve fitting, the collected data were processed using INRIM's CCC Software employing nonlinear regression techniques [12,13]. Fig. 3 presents both the raw calibration data and the resulting fitted calibration curve:

The calibration curve was used to correct the raw flow measurements, enabling a more precise determination of the actual flow rate and, consequently, the cumulative volume delivered. This total volume was calculated by applying the trapezoidal numerical integration method.

To evaluate how the choice of flow rate might affect the accuracy of the measurements, a series of experiments was conducted where the same pressure increase was achieved using nominal flow rates of 1, 2, and 4 SCCM for the Microgas and 4000 SCCM for the Megas. Although the detailed results are not shown here, the tests demonstrated that variations in flow rate had minimal impact on the final outcomes. For the conclusive tests reported in Section 5 for the Microgas, a flow rate of 2 SCCM was selected as the best compromise: the highest flow rate (4 SCCM) involved shorter measurement times, increasing the sensitivity to transient effects during fluid delivery, while the lowest flow rate (1 SCCM) produced slightly higher uncertainties in flow measurement.

4.2. Uncertainty analysis

This subsection focuses on the analysis of measurement model Eq. (8), applying the uncertainty propagation techniques outlined in the GUM guidelines [10].

We will first present the overall analysis, which will be followed by the derivation of the various uncertainty contributions.

Drawing from the model Eq. (8) and applying the uncertainty propagation formulae for multiplicative models [10], it is easy to obtain that:

$$u^2(V) = u^2(V_{add}) + u^2\left(\frac{p_{ref}}{T_{ref}}\right) + u^2(T_f) + u^2(p_f) + u^2\left(\frac{1}{1 - \frac{p_i}{p_f} \cdot \frac{T_f}{T_i}}\right) \quad (9a)$$

It can be observed that the sensitivity coefficients of all terms correspond to 1; the probability distribution is considered as normal in all cases due to the origin of the contributions.

4.2.1. Contribution from the added volume V_{add}

This component was assessed using the integration uncertainty estimation approach outlined in [12], which we briefly summarize here. The total delivered volume is of course the integral of the flow rate along the acquisition period, which due to the fact that the flow rate value is acquired at discrete intervals can be expressed in finite form as:

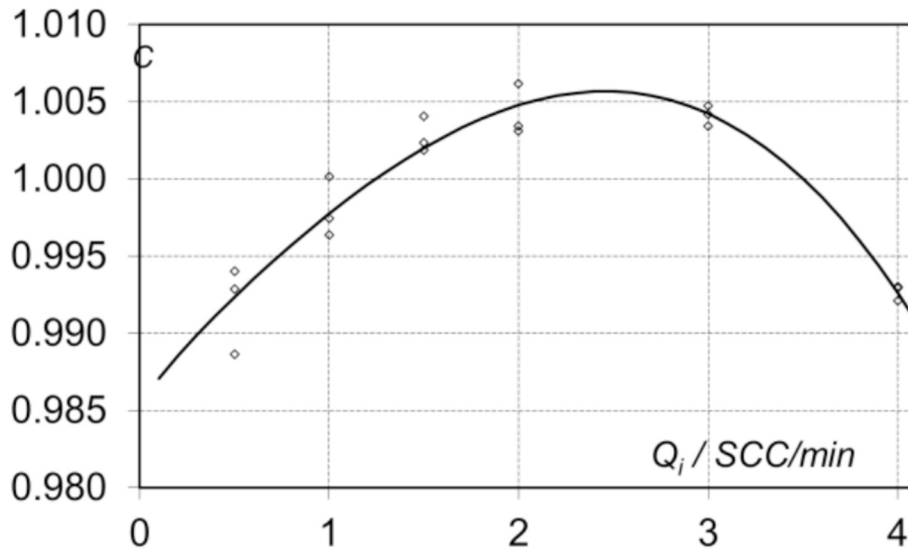


Fig. 3. Calibration of the mass flow controller used in the microgas experiments.

$$V_{add} = \sum_{i=1}^N V_i = \sum_{i=1}^N \underline{Q}_i \delta t_i \tag{9b}$$

where V_i are the contributions of the partial volumes to the integral, \underline{Q}_i the average of the flow rate across a time interval and δt_i the duration of the time interval. Eq. (9a) can be expressed in matrix form in order to account for the fact that the same flowrate discrete value contributes to the uncertainty of two adjacent partial volumes. It is shown in [12] that, in the case of approximately constant flowrate, the uncertainty in the integrated volume can be expressed as:

$$u^2(V_{add}) \approx \underline{Q}^2 u_{\delta t}^2 + (2N - 1) \delta t^2 u_r^2 + 4\Delta t^2 u_c^2 \tag{10a}$$

where Δt is the acquisition period, u_r is the random fluctuation of the flowrate measurement and u_c is the calibration uncertainty (correlation term) of the instrument.

Notice that Eq. (10a) is an approximation in closed form of the complete evaluation which implies matrix operations on the vectors of acquired flowrate and measurement times; we performed such operations via a suitable software, using the following parameters:

- Time uncertainty of 1 ms, rectangular distribution (for both pistons)
- MFC resolution of 0.001 SCCM(Microgas); 0.01 SLM (Megas)
- Flowrate uncertainty from scatter of the MFC signals (for both pistons).
- Correlation between flow rate measurements corresponding to the calibration reference uncertainty, i.e. 0.05 % (for both pistons).

The resulting uncertainty $U(V_{add})/V_{add}$ was found to be in all cases of about 0.2 % (for both pistons).

4.2.2. Contribution from the term T_f

This term's contribution is influenced by the measurement uncertainties of the instrument used for temperature measurements, for which the uncertainty assessment includes the following components (for both pistons):

- calibration uncertainty of the thermometers, corresponding to 0.015 K (small piston) / 0.025 K (large piston) (Gaussian distribution);
- resolution uncertainty of the thermometer, 0.01 K (rectangular distribution, both cases);
- fluctuation during the measurement, typically 0.02 K (rectangular distribution, both cases).

These components were summed in quadrature, providing a total

uncertainty of 0.027 K (small piston) / 0.034 K (large piston), or in percentage terms 0.009 % / 0.011 %.

4.2.3. Contribution from the term p_f

Correspondingly, for the barometer the following values were considered:

- calibration uncertainty of the barometer, corresponding to 5 Pa (Gaussian distribution);
- resolution uncertainty of the barometer, 0.1 Pa (rectangular distribution);
- fluctuation during the measurement, typically 1 Pa (rectangular distribution).

Hence a total pressure uncertainty of 5.2 Pa, or 0.005 %. This value was increased to 0.015 % in the case of the large piston for the reasons discussed in section 5.2.

4.2.4. Contribution from the term $\frac{1}{1 - \frac{p_i}{p_f} \frac{T_f}{T_i}}$

The contribution from this term can be divided into two main parts. Initially, the pressure and temperature contributions are evaluated. The pressure and temperature terms are analyzed similarly to the previous sections, yielding the same outcome, both for initial and final conditions since identical instruments are employed. These two measurements are treated as independent, allowing the percentage uncertainties to be combined using the root-sum-square method, which yields a total uncertainty of 0.014 %. Conversely, the experimental values of the expression $\frac{p_i}{p_f} \cdot \frac{T_f}{T_i}$ are very close to unity; thus, even a minor percentage uncertainty can significantly affect the overall uncertainty. For instance, if $\frac{p_i}{p_f} \cdot \frac{T_f}{T_i} = 0.98$, the absolute uncertainty would be 0.00014. This uncertainty also applies to the entire term, which has an absolute magnitude of 0.02, resulting in a relative uncertainty of 0.75 %. This represents the largest contributor to total uncertainty and is strongly influenced by the ratio between the initial and final pressures¹. One effective method to reduce this source of uncertainty is to increase the pressure differential between the starting and ending conditions.

4.3. Uncertainty of the dead volume V_f

It is now possible to combine the various uncertainty contributions as expressed in Eq. (9a), which brings to the following tables:

5. Results and discussion

The data collected following the methodology outlined in Section 4 are presented in this section, together with the results derived from their in-depth analysis.

5.1. Data set description

The added volume was determined using an MKS Mass Flow Controller (MFC) with a maximum capacity of 5 SCCM (small piston case) or 20,000 SCCM (large piston case), which was operated through specialized software. This application allowed configuration of MFC settings, establishment of steady-state flow, activation of flow delivery, and logging of the signal at predetermined intervals. Prior to testing, the MFC underwent rigorous calibration on the test rig. Our standard protocol involved conducting seven calibration points, each repeated three times, to ensure both accuracy and repeatability. To derive accurate calibration curves, the collected measurements were processed using INRIM's CCC Software with nonlinear regression methods [14,15,16]. Fig. 3 presents an example of raw calibration points alongside the resulting best-fit curve (5 SCCM MFC case). Regarding the measurements about the large piston prover, two sets of tests were performed; in analogy to the other case, the first set was performed by adding gas at the lowest possible position of the piston (5 measurements), while the second set concerned the addition of gas with the piston lifted by about 14 mm, corresponding to 10.22 L (3 measurements).

5.2. Rough measurement

In this section some examples of the measurements of pressure, temperature and flow rate are described in detail for both the facilities.

Figs. 4a,b and 5a and b display typical examples, respectively, of the temperature and pressure recorded during a single measurement:

The observed temperature remained highly stable—fluctuating by less than 0.01 K throughout the measurement. Pressure, on the other hand, was steady before and after the gas injection, but exhibited a predictable, continuous rise during the MFC-driven flow.

It can be observed in Fig. 5b that the pressure displays a peak value at the end of the injection, followed by a slow relaxation; we speculate that this can be due to a thermal relaxation of the gas entering the piston, but more analysis on the phenomenon will be needed to confirm this hypothesis; of course, this fact implies that the final reading of the pressure in the large piston is less accurate than in the case of the small piston, which was accounted for in the computations by increasing the pressure uncertainty; this is one of the reasons why the overall uncertainty is larger in the case of the large piston (see Tables 1 and 2).

To illustrate this pressure behavior more clearly, Fig. 6 presents an

enlarged section of the final part of the data shown in Fig. 5a:

The pressure remains remarkably stable—fluctuating by only a few tenths of a Pascal—which confirms both the effectiveness of the piston seal and the accuracy and consistency of our pressure measurement system. Meanwhile, Figs. 7a and b illustrate the flow rates recorded during two example experiments in the two pistons.

It can be observed that the flow rate, in most of the measurement run, is very stable; on the other hand, both the initial and final transients display slight overshoots, which, albeit being considered in the integration phase, can provide some disturbance to the overall measurements; in order to minimize this disturbance, it was decided to perform measurements having a duration of at least 120 s.

In reference to the second test case (large piston), the behaviour of pressure, temperature and flow rate is essentially the same, the main differences being the following:

- The temperature stability is slightly lower, which is coherent with the much larger volume and the slightly higher uncertainty associated to the temperature measurement;
- The pressure stability required more time to be reached at the final measurement;
- The flow rate fluctuation during the constant flow is similar to the one already shown, albeit slightly higher;

Altogether, these differences cause a slight increase in the overall uncertainty of the measurement, which is reflected in the higher uncertainty that was presented in Section 4.3.

5.3. Results elaboration

The datasets described in Section 5.2 were further processed to estimate the dead volume following the approach detailed in Section 3, and the associated uncertainty was calculated as per the methodology in Section 4. The summarized outcomes are presented in Table 1a (small piston) and Table 2 (large piston). A key finding is that, in every case reported in Table 1b, the uncertainty in the calculated dead volume is significantly below the previously applied uncertainty of 7.9 mL (see Section 2.1) for the case of the small piston, and correspondingly for the large piston. This striking reduction—nearly fourfold—validates the robustness of our method. Furthermore, for the experiments involving the differential pressure transducer (tests #1, #3, and #5), the determined dead volume values align closely with the reference volume of 262 mL, confirming consistency across configurations.

Another observation that can be made is that the results obtained in corresponding cases are well compatible with each other, and that the uncertainty in all cases is essentially the same; the small deviations between the measurements presumably are due to a small zero-drift

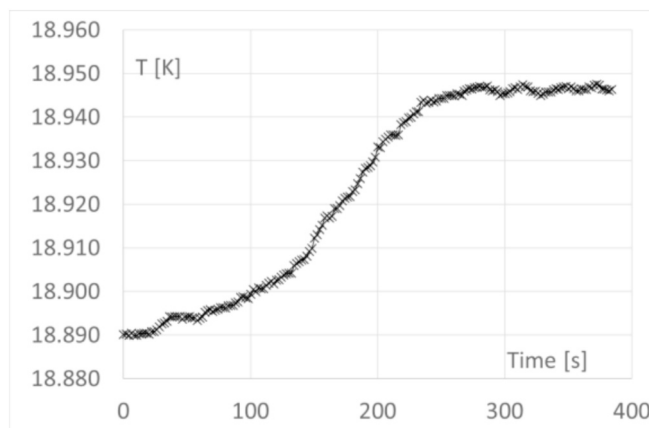
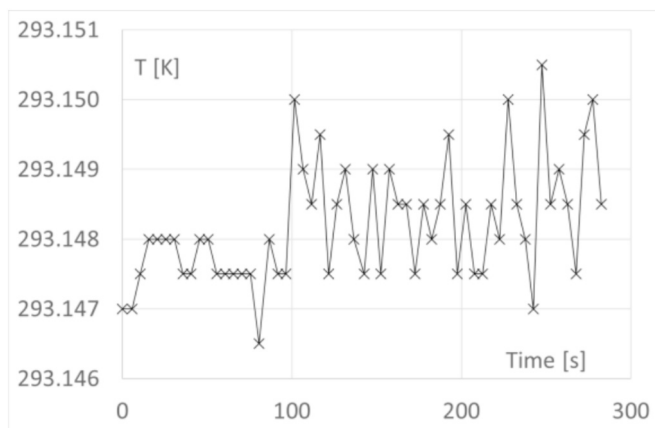


Fig. 4. a. small piston, temperature recorded during measurement run #2. b. large piston, temperature recorded during run #4.

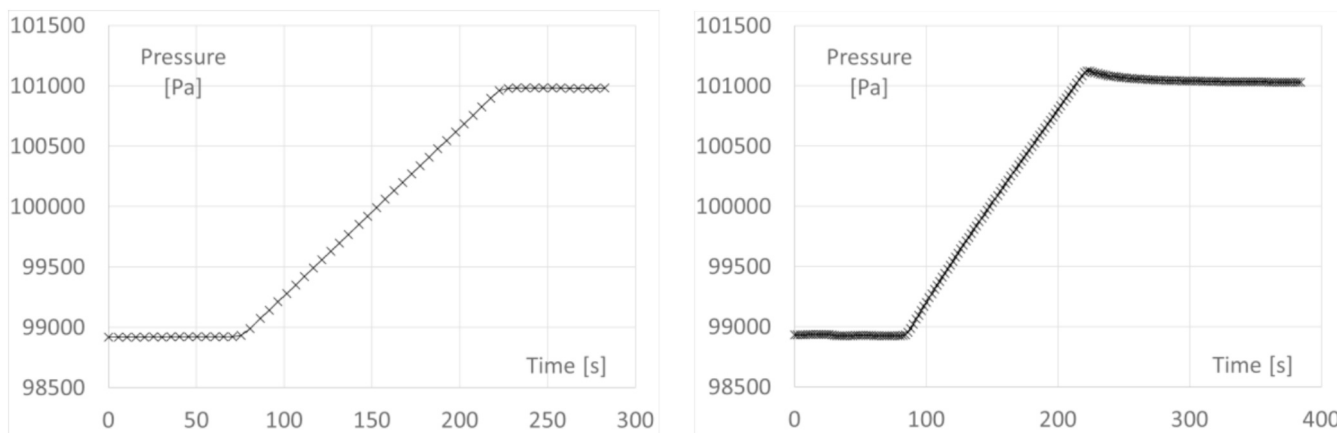


Fig. 5. a. small piston, pressure recorded during measurement run #2. b. large piston, pressure recorded during run #4.

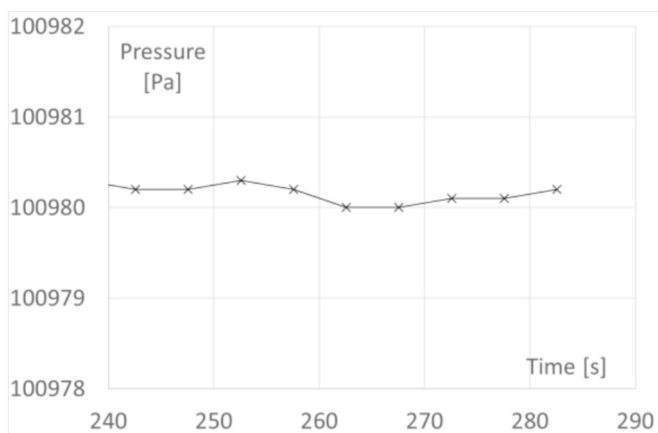


Fig. 6. Detail from Fig. 5a.

effect that was observed on the MFC during measurements.

Regarding the results pertaining to the large piston, it can be observed that, also in this case, the different test cases provide results which are fully compatible, not only between them but also with the geometrical evaluation data. Again, the uncertainty of the new evaluation method is convincingly lower than the previous version (although the reduction in uncertainty is not as large as in the case of the small piston), thus showing the advantage of the method.

The consistency of the results in all tests shows that the method is

reliable and therefore, after another round of tests for check and verification, such results will be applied to the piston prover at INRIM as follows:

- small piston prover: from the data at hand, the expected value of dead volume to be applied is considered to be 261 mL with an associated uncertainty of 1 % (increased with respect to the computed value for safety) in the case of the baseline configuration, and 243 mL associated to the same relative uncertainty in the case when the pressure transducer is not connected;
- large piston prover: for this test rig, we consider to apply a dead volume estimate of 454 L with an associated uncertainty of 1.5 %, or 6.8 L, again increased for safety with respect to the value obtained from computation.

The impact of these modifications will be quite reduced in itself but, in conjunction with other improvements in progress for our test rigs (e.g. [5]), should bring the overall uncertainty of the devices to a measurable reduction, which will be inserted in the laboratory CMCs once validated.

As an example, the current uncertainty budget for the small piston prover is detailed in Table 3; notice that this budget considers only the uncertainty components associated to the test rig, neglecting the components associated to the DUT (Device Under Test) and the scatter between repetitions. This Table takes into account an unfavourable but possible scenario, in which the density variation during the test is relatively high (0.1 %, corresponding e.g. to a pressure variation of about 100 Pa, which is a value that was actually observed during long runs); it can be observed that the main uncertainty components are

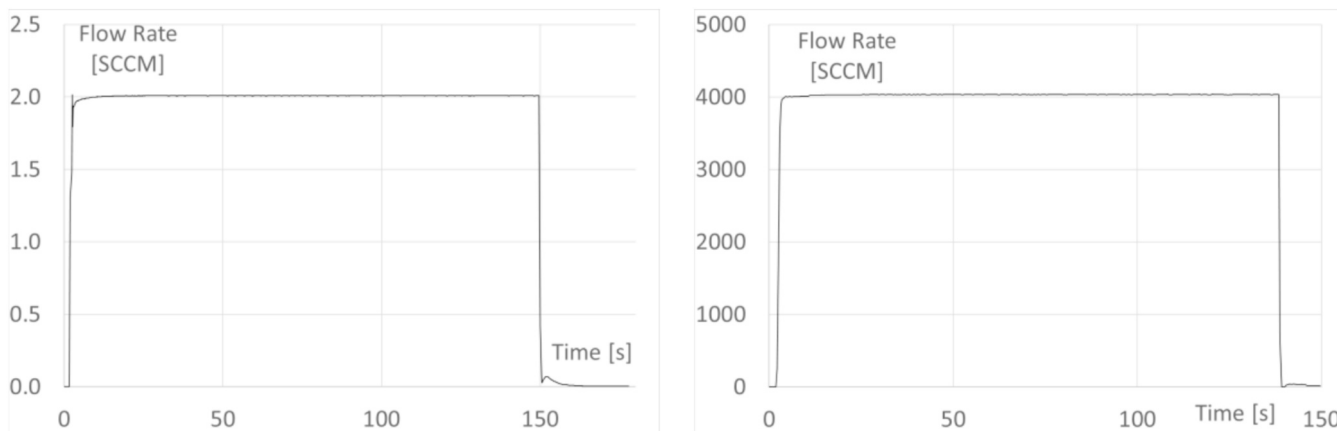


Fig. 7. a. small piston, flow rate measurements during run #2, nominal flow rate 2 sccm. b. large piston, flow rate measurements during run #4, nominal flow rate 4000 sccm.

those associated to the volume variation and to the initial volume, and that the two are of the same magnitude. The final result is a standard uncertainty of 0.016 % for the measurement performed by the piston; when adding the uncertainty components associated to the DUT and a typical scatter, this brings to an expanded uncertainty of 0.05 %, which is the CMC (Calibration and Measurement Capability) of the test rig described here.

In table 4, on the other hand, the same computation is repeated using the dead volume reduced uncertainty. It can be observed that, in this case, the component associated to the initial volume is reduced to a fraction of the volume variation uncertainty, allowing therefore to bring the standard uncertainty associated to the measurement performed by the piston to 0.012 %, i.e. a measurable reduction of this component. Of course, this effect can be appreciated because of the small value of the overall uncertainty and would not be so evident in a piston with higher uncertainty, e.g. it would presumably become immaterial for a test rig with an overall uncertainty of 0.2 %.

6. Conclusions

This study introduced an experimental approach for accurately determining the dead volume in sealed systems. While the underlying principle is straightforward, its effective implementation necessitates precise thermodynamic measurements and meticulous control over the added gas volume, which is central to the method's accuracy. The findings demonstrate that, when appropriately applied, this method can reduce the uncertainty associated with dead volume by a factor up to three. Nevertheless, integrating this method with efforts to address other uncertainty factors is anticipated to contribute to a reduction in the overall uncertainty reported in CMCs. Future work includes conducting a new series of measurements to validate the results presented herein and to improve the implementation details in order to optimize the results.

Credit authorship contribution statement

Pier Giorgio Spazzini: Writing – review & editing, Writing – original draft, Investigation, Formal analysis, Data curation, Conceptualization. **Aline Piccato:** Writing – review & editing, Writing – original draft, Investigation, Formal analysis, Data curation.

Declaration of competing interest

The authors declare that they have no known competing financial interests or personal relationships that could have appeared to influence the work reported in this paper.

Acknowledgments

The Authors wish to thank Mr Gaetano la Piana and Mr Marco Santiano, who supported the initial development and the diffusion of the research presented in this paper.

Data availability

Data will be made available on request.

References

- [1] Xxxxx: undisclosed for anonymity.
- [2] G. Cignolo, A. Rivetti, G. Martini, F. Alasia, G. Birello, G. La Piana, The national standard gas provers of the imgc-cnr, in: *Proceedings of the FLOMEKO 2000*, 2000, p. 8.
- [3] F. Berg, G. Cignolo, NIST-IMGC comparison of gas flows below one litre per minute, *Metrologia* 40 (2003) 154–158.
- [4] G. Cignolo, F. Alasia, A. Capelli, R. Gorla, G. La Piana, A primary standard piston prover for measurement of very small gas flows: an update, *Sens. Rev.* 25 (1) (2005) 40–45.
- [5] P.G. Spazzini, A. Piccato, P. Pedone, **Reduction of a Gas Prover Uncertainty**, Proceedings of the 10th International Symposium on Fluid Flow Measurement (ISFFM), Queretaro, Mexico, 2018.
- [6] A. Piccato, M. Bisi, P.G. Spazzini, F. Bertiglia, G. La Piana, E. Audrito, M. Santiano, R. Bellotti, C. Francese, Metrological features of the large piston prover at INRIM, *Measurement* 192 (2022) 110841, <https://doi.org/10.1016/j.measurement.2022.110841>.
- [7] J.D. Wright, A.N. Johnson, M.R. Moldover, Design and uncertainty analysis for a pvtt gas flow standard, *J. Res. Nat. Inst. Stand. Technol.* 108 (2003) 21–47. ISSN 1044-677X.
- [8] F. Boineau, M.D. Plimmer, E. Mahé, Volume calibration using a comparison method with a transfer leak flow rate, *Acta IMEKO* 9 (5) (2020) 70–75, https://doi.org/10.21014/acta_imeko.v9i5.997.
- [9] J. A. Bocanegra, F. Scarpa, V. Bianco, L. A. Tagliafico, **The effect of dead volumes on the performance of magnetic refrigerators**, *International Journal of Refrigeration*, Vol. 151, pp. 26-38, 2023, ISSN 0140-7007.
- [10] V. Grosfils, R. Hanus, A. Vande Wouwer, M. Kinnaert, Parametric uncertainties and influence of the dead volume representation in modelling simulated moving bed separation processes, *J. Chroma. A* 1217 (47) (2010) 7359–7371, <https://doi.org/10.1016/j.chroma.2010.09.030>.
- [11] J. Wright, A. Johnson, M. Moldover, S. Nakao, Gas flow standards and their uncertainty, *Metrologia* 60 (1) (2022), <https://doi.org/10.1088/1681-7575/ac8c99>.
- [12] P.J. Davis, P. Rabinowitz, *Methods of Numerical Integration*, 2nd ed., Academic Press, USA, 1984.
- [13] BIPM, IEC, IFCC, ILAC, ISO, IUPAC, IUPAP, OIML, **Evaluation of measurement data - Guide to the expression of uncertainty in measurement**, Joint Committee for Guides in Metrology, JCGM 100:2008, 2008.
- [14] P.G. Spazzini, W. Bich, Uncertainty in discrete-time integration — the case of static gas meters, *Measurement* 224 (2024) 113821. ISSN 0263-2241.
- [15] M. Lecuna, F. Pennecchi, A. Malengo, P.G. Spazzini, Calibration curve computing (CCC) software v2.0: a new release of the INRIM regression tool, *Meas. Sci. Technol.* 31 (11) (2020) 114004.
- [16] A. Malengo, F. Pennecchi, P. G. Spazzini, **Calibration Curves Computing – CCC software**, available for download at <http://www.inrim.it/download/CCC/index.html>, Release 1.3, June 2015.